Journal of Hydrology: Regional Studies 42 (2022) 101149

Contents lists available at ScienceDirect

Journal of Hydrology: Regional Studies

journal homepage: www.elsevier.com/locate/ejrh

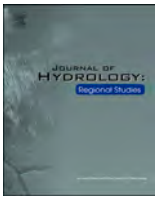

# Assessment of traditional rainwater harvesting system in barren lands of a semi-arid region: A case study of Rajasthan (India)

Basant Yadav [a], Nitesh Patidar [b], Anupma Sharma [b], Niranjan Panigrahi [c], Rakesh K. Sharma [d], V. Loganathan [e], Gopal Krishan [b], Jaswant Singh [f], Suraj Kumar [b], Alison Parker [c,*]

[a] Department of Water Resources Development and Management, Indian Institute of Technology Roorkee, 247667, India
[b] National Institute of Hydrology, Jal Vigyan Bhavan, Roorkee 247 667, India
[c] School of Water, Energy and Environment, Cranfield University, Cranfield Mk43 0AL, UK
[d] Department of Chemistry, Indian Institute of Technology Jodhpur, Jodhpur 342037, India
[e] Department of Civil Engineering, Indian Institute of Technology Roper, 140001, India
[f] Department of Hydrology, Indian Institute of Technology Roorkee, 247667, India

ARTICLE INFO

*Keywords:*
Rainwater harvesting
Groundwater recharge
Semi-arid regions
HYDRUS

ABSTRACT

*Study region:* Dudu station, Rajasthan, India
*Study focus:* Rainwater harvesting can be used as a method to recharge aquifers. This can happen with a variety of scales and technologies. One such example is shallow infiltration ponds (*Chaukas*) which recharge groundwater and increase soil moisture facilitating pastureland development. A HYDRUS-1D model was used to estimate potential groundwater recharge. The model was calibrated using field data from 2019 and validated using data from 2020. The time series of Normalized Difference Vegetation Index (NDVI) was derived at annual scale to assess changes in the vegetation cover.
*New hydrological insights for the region:* The modeling revealed that an additional 5% of the rainfall depth was being recharged into the groundwater. In addition, the additional soil moisture was allowing natural grass cover to develop, which could be used by the local community as pastureland. These twin benefits that the local communities are realizing could be scaled up beyond Dudu, to India, and worldwide, as many regions have barren land that is slightly sloping, together with permeable soils, which are the only conditions for the construction of *Chaukas*. These *Chauka* systems have helped in sustainable water resources management in these water-stressed regions and the additional livelihood support through developed pastures for animal husbandry.

## 1. Introduction

The development of life on earth and human progress depends strongly on the availability and use of water, and globally, the freshwater resources like groundwater contribute significantly in meeting the demands of domestic and agricultural water. (Villholth, 2006). Over 55% of India's population, which is the home to 15% of the global population, relies on groundwater for an array of

* Corresponding author.
*E-mail address:* a.parker@cranfield.ac.uk (A. Parker).

https://doi.org/10.1016/j.ejrh.2022.101149
Received 9 September 2021; Received in revised form 17 June 2022; Accepted 18 June 2022
Available online 25 June 2022

different activities, such as irrigation, water for cattle, domestic consumption, and industrial uses (Moriarty et al., 2004). In India, groundwater use saw rapid growth since the 1950 s, soaring from 20 $km^3year^{-1}$ to 251 $km^3year^{-1}$in 2010 (Shah, 2007; Food and Agriculture Organization, 2016), making it the world's greatest groundwater abstracter, surpassing the USA and China combined (Food and Agriculture Organization, 2016). It is estimated that India generates 9% of its GDP from groundwater abstraction (Mudrakartha, 2007). As it is more flexible and reliable than the public water service, 85% of the rural population and 60% of the irrigated agriculture have become dependent on groundwater. This trend has been bolstered by decreasing capital costs and generous public energy subsidies (World Bank, 2010). Because of this ever-increasing use of groundwater, the Central Ground Water Board (CGWB) classified 16% of India's aquifers as overexploited and an additional 3% as in a critical state (CGWB, 2017). Sheetal (2012) reported local water table level drop by up to 16 m between 1980 and 2010, while Sarah et al. (2014) mentioned, in several states, decline rates of 1–2 $myear^{-1}$ since 2000. Such declines impact small-scale farmers relying on groundwater for irrigation (Singh et al., 2002; Zaveri et al., 2016). Furthermore, the declining water table has led to the deterioration of groundwater quality in many locations (Coyte et al., 2018). Panda et al. (2020) cite India as an example of surface greening and subsurface drying. As signs of aquifer over-exploitation started to accumulate in the 1960 s, Managed Aquifer Recharge (MAR), or Artificial Recharge, emerged to alleviate some of the pressure on the groundwater resources (Sakthivadivel, 2007).

In India, where rainfall patterns are highly variable, rainwater harvesting has been used for centuries. Applied to MAR, the principle is to store a fraction of the vast runoff volume generated during the monsoon, increasing its residence time and allowing it to percolate into depleted aquifers. It has received growing attention from governmental and civil institutions and was included in the central government policies on groundwater management in the 1990 s (Sakthivadivel, 2007). In the latest version of its Master Plan for Artificial Recharge to Ground Water, the CGWB (2013) highlighted the ambitions to build a total of 11 million recharge structures with a recharge capacity of 85.5 billion cubic meters per year. This would account for 34% of India's total groundwater abstraction in 2010 (FAO, 2016). Many different structures can be built for rainwater harvesting in arid to semi-arid environments. Check dams (small dams typically built, in MAR application, across ephemeral rivers) are among the most common, with the CGWB (2013) aiming to develop almost 300,000 of them. Very localized solutions also exist, such as the shallow infiltration ponds *(Chaukas)* in Rajasthan, a system developed by a local community organisation, Gram Vikas Navuyak Mandal Lapodiya (GVNML).

Practitioners consider that the main hydrological impact of *Chaukas* is to increase and maintain soil moisture rather than

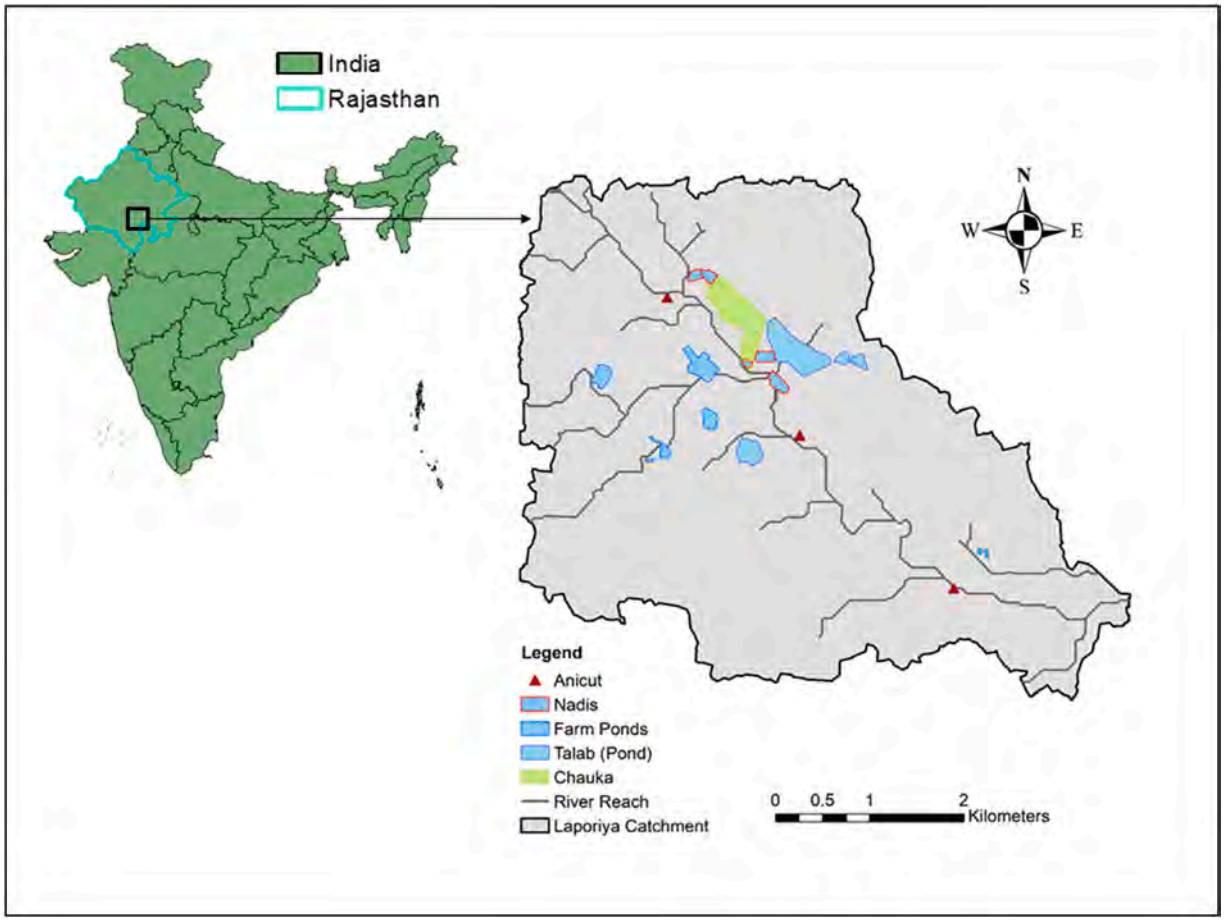


**Fig. 1.** Study area along with the types of rainwater harvesting structure in the Lapodiya catchment.

recharging the aquifer themselves (Gram Vikas Navuyak Mandal Lapodiya, 2007). This increase, combined with seeding, provides the community with grazing areas for several months a year, increasing pastureland and supporting livelihoods. Additional benefits include erosion control, an increase in biodiversity, and an improved living environment (GVNML, 2007). However, the size of locally managed aquifer recharge structures is small, resulting in limited water holding capacity, and hence the contribution to the groundwater recharge may not be significant (Sharda et al., 2006). Therefore, they may not be reliable in drought years and may not provide additional benefits in catchments with other larger MAR structures (Kumar et al., 2008).

On the other hand, rainwater harvesting using these small structures can redistribute the harvested rainwater in the catchment by converting the excess runoff into recharge, consequently altering the variables like evaporation, soil moisture and streamflow in the total water balance (Glendenning and Vervoort, 2010). Various rainwater harvesting methods have been studied to understand their hydrological impacts on the surrounding aquifers (Badiger et al., 2002; Neumann et al., 2004; Gontia and Sikarwar, 2005; Sharda et al., 2006; Stiefel et al., 2009; Scanlon et al., 2009). A holistic assessment of the chaukas was carried out by Everard and West (2021) but their study relied on interview and remote sensing data rather than any field data. Thus there has not been any study on the recharge potential of the chuakas. In this study the objectives are to quantify the recharge potential of these shallow infiltration ponds in barren lands and to determine their impact on vegetation cover.

## 2. Study area

Rajasthan is a northern state in India, also known as the desert state of India, has an area of 342,239 $km^2$, which is 10.4% of India's

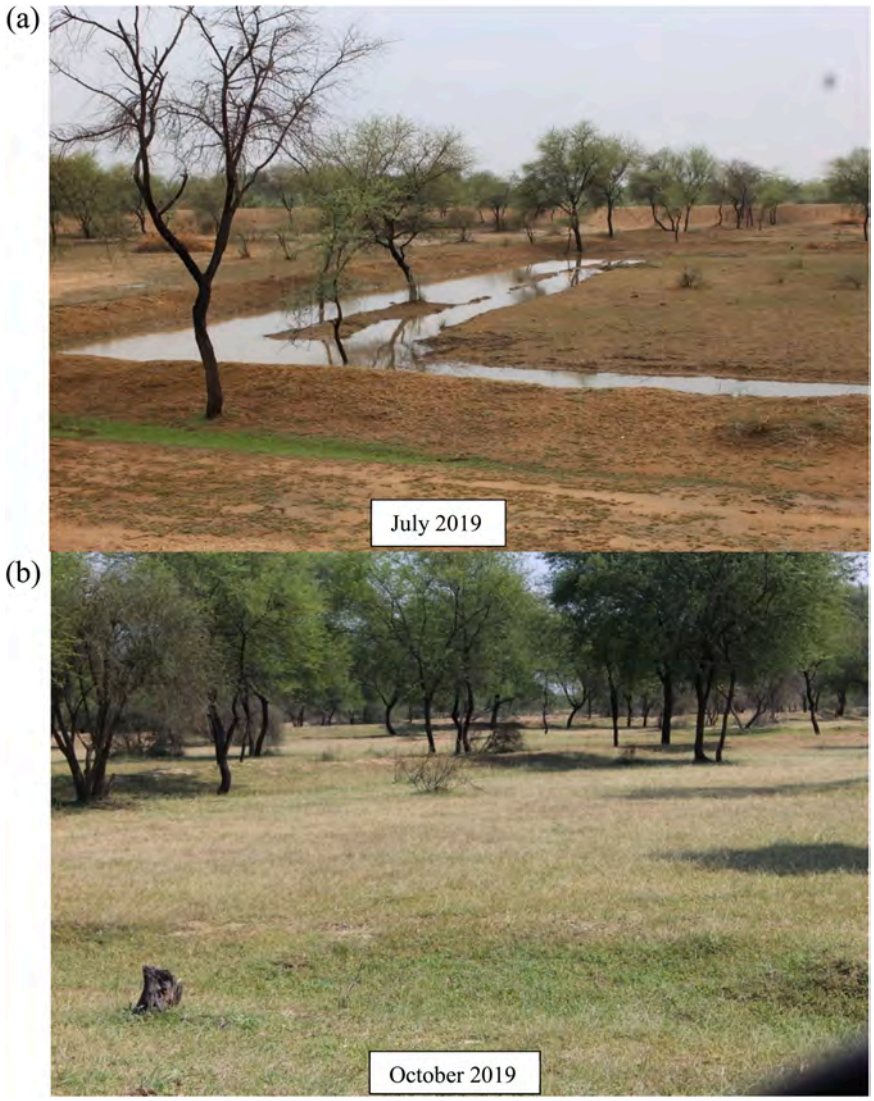


**Fig. 2.** *Chauka* system in the (a) monsoon season of 2019 and (b) post-monsoon season of 2019.

total geographical area. It is the largest state in Indian by area and ranked 7th in the population of the country. The majority of Rajasthan terrain is barren and lacks vegetation coverage, which indicates little water present. The soil types in Rajasthan are mostly sandy, loamy, saline, alkaline, and chalky (calcareous). The majority (91%) of the population's drinking water is groundwater, and 66% of the aquifers in Rajasthan are overexploited (CGWB, 2012).

Due to water shortage, various rainwater harvesting structures were installed to harness rainwater in the Lapodiya catchment. Fig. 1 shows a map of the Lapodiya catchment depicting the different water harvesting structures such as Farm ponds, *Talab*(ponds), *Chauka* system, *Nadis* (small ponds), and *Anicut* (check dams). In this region, rural villages with pastoral characteristics have a small population that practices mainly agricultural activities such as crop cultivation and animal husbandry as their means of survival. A Non-Governmental Organization (NGO), Gram Vikas Navuyak Mandal Lapodiya (GVNML), implemented a *Chauka* and *Nadis* system to take on water quantity and quality problems. *Chauka*s are infiltration ponds developed locally to support pastoral lands in the early dry season. The ponds store catchment runoff, while the check dams act as a barrier to reduce the amount of river water from flowing out of the catchment. During the monsoon season, the excess rainwater from *Chauka* and ponds flows into the river. This seasonal river meets a larger dam downstream that provides water to many districts in Rajasthan. This network of ponds, check dams, and *Chauka* systems harness the rainwater during the monsoon season for future use. At the same time, they maintain the soil moisture at a satisfactory level for pasture growth. GVNML proactively network with the residents to mobilise, supervise, and coordinate their effort better to manage the water resources with the pond system so that their agricultural activities can be sustainable. Rainwater harvesting using these traditional and modern structures has been considered helpful by local people in developing the pasturelands and enhancing groundwater recharge. However, such claims have not been proven scientifically in this region.

The climate in Lapodiya catchment is typical of a semi-arid region with hot summers commencing in March and continuing until June. The mean maximum temperatures in this region reach as high as $48^0$ C in June, while the temperatures drop in January between $7.7^0$ C and $21^0$ C (CGWB, 2015). The state receives maximum rainfall (90% of the total rainfall) in the monsoon season (June-September), which is the primary source of groundwater recharge. The average yearly rainfall and annual potential evapotranspiration in the Jaipur district is 575.7 mm (1971–2014) and 1477.7 mm, respectively (CGWB, 2017).

The *Chaukas* in the Lapodiya catchment is a unique RWH system developed indigenously by a local community organisation, GVNML. The *Chauka* forms an enclosure about 2000 $m^2$, built across a gently sloping area by placing earthen dykes on the sides. One *Chauka* trench can contain up to 25–30 cm of water when it is filled. Fig. 2 shows the *Chauka* system's conditions during the monsoon season (Fig. 2a) and post-monsoon season (Fig. 2b) of 2019. They are designed to hold little runoff water that slowly infiltrates in the soil and are built-in series so that when one *Chauka* gets filled, it will overflow to the adjoining *Chaukas*. The excess water from the *Chaukas* flows to the nearby *Nadi* or *Talab*. Practitioners consider that the main hydrological impact of *Chaukas* is to increase and maintain soil moisture rather than recharging the aquifer themselves.

Uncontrolled grazing in the study area has left the pastures completely denuded of perennial grass cover, frequently replaced by annual unpalatable grasses, and ultimately reduced to almost bare soil. Under such circumstances, Aristida sp. (locally known as *lapla*) is the only vegetation that predominates (GVNML, 2007). Community lands were the source of the people's basic livelihood, especially the poor; therefore, pasture improvement and plantation strategies were followed to rejuvenate the lost pasturelands. Soil moisture conservation through rainwater harvesting in the *Chauka* system provides essential water for plant growth in the semi-arid region of Lapodiya. The development of the *Chauka* system in the barren land of Lapodiya was done with the aim to convert this wasteland into a pastoral land.

The regional lithology prepared by CGWB suggest that aquifers in this region comprise hard rocks of the Bhilwara Super Group, comprising granulitic gneisses, quartz mica schist, phyllite, and granite pegmatite intrusive (CGWB, 2013). The presence of fine sand, silt and clays, and banded gneiss found at varying depths accompanied by weathered and fractured zones. Banded gneiss mainly consists of light and dark bands of quartz and feldspar and also contains biotite, hornblende and garnets. Weathered gneiss in the study area is made up of clay minerals including Potassium Iron Magnesium Aluminum Silicate Hydroxide, as well as sand particles. In these aquifers, groundwater movement is controlled by the pore size, continuity, and interconnectivity of weathered and fractured parts. As the primary porosity is very poor, secondary porosity in weathered and fractured parts is important. Groundwater in the Lapodiya region occurs both in the weathered zone and bedrock in unconfined conditions. Similar, geological profile with the depth of the Lapodiya catchment is given in Table 1.

**Table 1**
Geological profile with a depth of Lapodiya catchment.

| Depth (m) | Geology | Source |
|---|---|---|
| 0–1 | Sandy loam and loam soils | Rajasthan Ground Water Department (2008) |
| 1–20 | Weathered gneiss | CGWB (2017) |
| 20–40 | Schist mixed with mica, quartz, and feldspar pieces | CGWB (2017) |
| From 40–80 | Bhilwara Super Group, comprising of granulitic gneisses, quartz mica schist, phyllite along with granite and pegmatite intrusives | CGWB (2017) |

## 3. Methodology

### 3.1. Monitoring network development and data collection

The Lapodiya catchment was identified for conducting detailed studies of the *Chauka* system from 2019 to 2020. The *Chauka* system presented in Fig. 3 is located around 1.5 km northeast of the Lapodiya village. A local observatory was established in the catchment to collect the daily data for rainfall, temperature, and evaporation. In addition, an automatic rain gauge, Class A evaporation pan, and thermometers were installed in Lapodiya village, which is around 1.5 km away from the *Chauka* system. Although this is not as close to the chauka system as would be ideal, it was in a secure compound so it could be regularly monitored. To understand the hydrogeology, one 12.7 cm or 5-inch diameter borehole (BH1), as shown in Fig. 3, was drilled in the study area using a down-the-hole drill (DTH rig), and sediment samples were collected at every one-meter interval.

Further, the BH1 was also monitored weekly for depth to water level ($D_w$) below ground level (bgl). $D_w$ was also observed on a weekly interval in BH1 between June 2019 to September 2020. In addition, a gypsum block sensor in conjunction with a watermark soil moisture meter was used to measure the soil moisture tension in the *Chauka* field during the monsoon period of 2019 and 2020. The sensors were installed at 30 cm and 60 cm depth in the center of a *Chauka*, which measures the soil water potential between 0 and − 200 kPa (0 and 200 centibars). Further, trial pits of 150 cm were dug to collect the soil samples at a depth of 30 and 60 cm, which were used for soil texture classification.

### 3.2. Potential groundwater recharge estimation using HYDRUS 1D

HYDRUS-1D model was used to simulate the water flow and root water uptake in the *Chauka* system (Šimůneket al., 2005), assuming that the soil is homogeneous and isotropic. It is also assumed that the liquid flow process does not get affected by the air phase, and the contribution of the thermal gradient is negligible in the water flow. The water flow in the system is based on the 1D Richards equation:

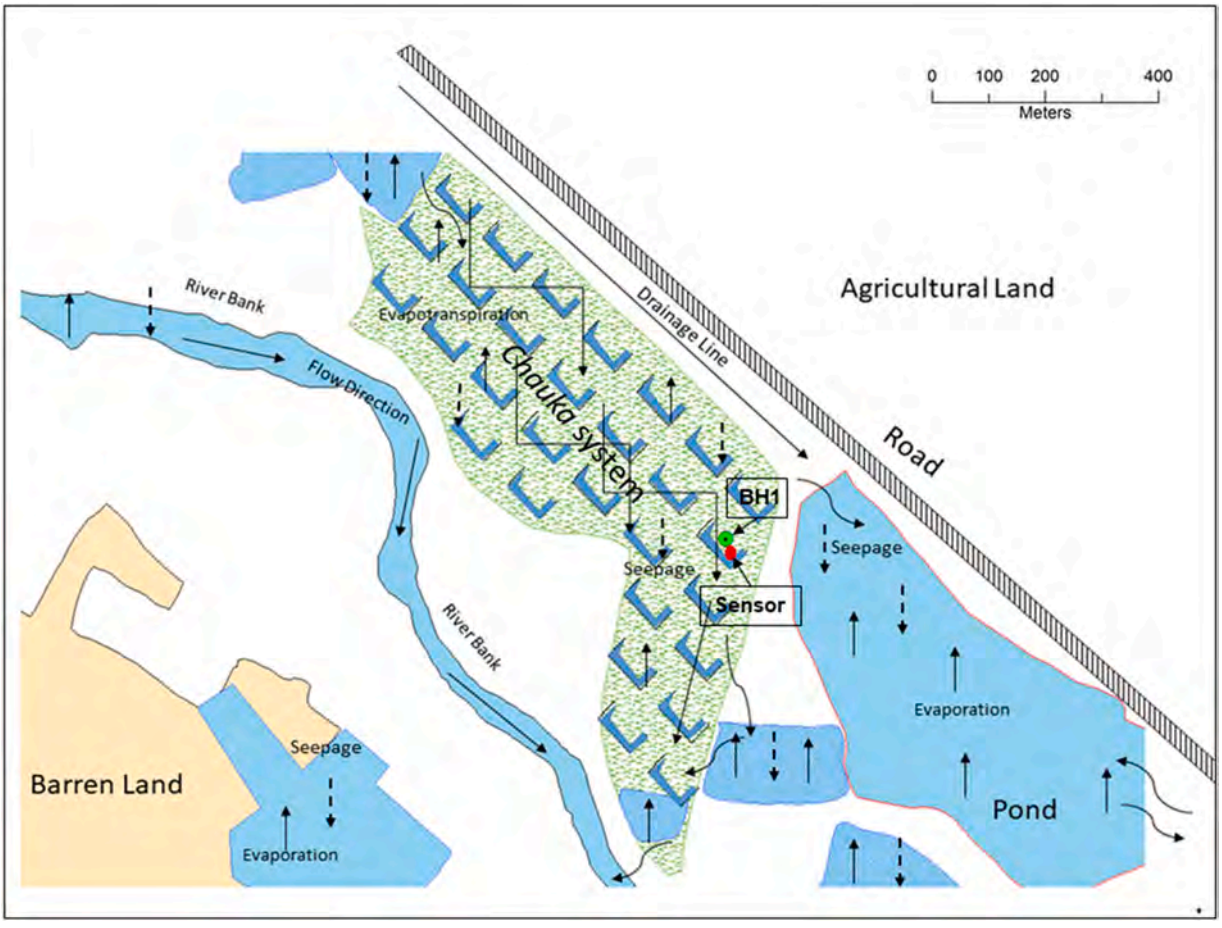


**Fig. 3.** Conceptual model of the *Chauka* system in Lapodiya showing the complex hydrology interaction of *Chauka* system with other recharge structures.

$$\frac{\partial \theta}{\partial t} = \frac{\partial}{\partial x}\left[K\left(\frac{\partial h}{\partial x} + 1\right)\right] - S \tag{1}$$

Where $h$ is the soil water pressure head (cm); $\theta$ is the volumetric water content ($cm^3 cm^{-3}$); $t$ is the time (d); $x$ is the spatial coordinate (cm); $K$ is the unsaturated hydraulic conductivity function (cm $d^{-1}$) and $S$ is the sink term ($cm^3$ $d^{-1}$), representing plant water uptake, which can estimated in terms of potential uptake rate and a stress factor (Feddes et al., 1978):

$$S(h) = \alpha(h) S_p \tag{2}$$

where $S_p$ is the potential root water uptake rate [$cm^3$ $cm^{-3}$ $d^{-1}$] and $\alpha(h)$ is the dimensionless water stress response function $(0 \le \alpha \le 1)$ which simulates the impact of soil moisture stress on the root water uptake. For $\alpha(h)$, we used the functional form introduced by Feddes et al. (1978):

$$\alpha(h) = \begin{cases} \dfrac{h - h_4}{h_3 - h_4}, & h_4 < h \le h_3 \\ 1, & h_3 < h \le h_2 \\ \dfrac{h - h_1}{h_2 - h_1}, & h_2 < h \le h_1 \\ 0, & h \le h_4 \; or \quad h > h_1 \end{cases} \tag{3}$$

Where $h_1$ and $h_4$ are the anaerobiosis and the wilting point above and below which root water uptake is null, respectively, $h_2$ and $h_3$ are the pressure heads between which root water uptake keeps the maximum rate. *Chauka* system is covered with natural grass during the rainfall season, and hence values for these parameters were taken from HYDRUS-1D database. (Šimůnek et al., 2005).

The soil water retention and soil hydraulic conductivity functions can be approximated using the van Genuchten–Mualem constitutive relationships (Mualem, 1976; Van Genuchten, 1980) as

$$\theta(h) = \begin{cases} \theta_r + \dfrac{\theta_s - \theta_r}{\left[1 + |\alpha h|^n\right]^{1-1/n}}, & h < 0 \\ \theta_s, & h \ge 0 \end{cases} \tag{4}$$

$$K(h) = K_s S_e^l \left\{1 - \left[1 - S_e^{n/(n-1)}\right]^{1-1/n}\right\}^2 \tag{5}$$

where $S_e$ is effective saturation:

$$S_e = \frac{\theta(h) - \theta_r}{\theta_s - \theta_r}$$

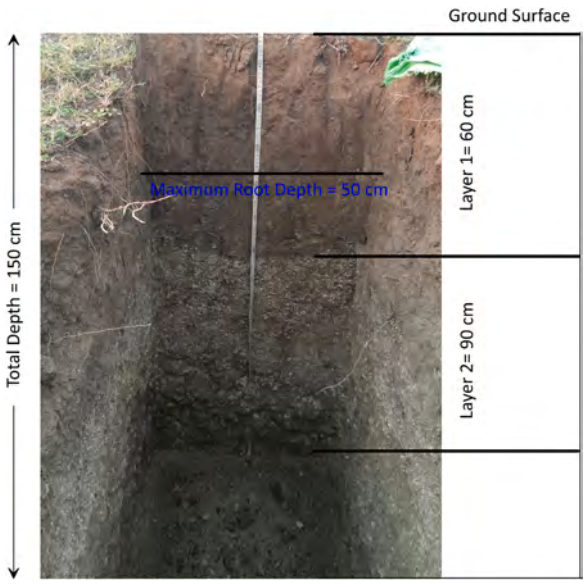


**Fig. 4.** Trial pit in the *Chauka* system and identified soil layers along with the maximum root depth in October 2019 (Note: Layers shown in this figure are different from the modeling layer).

where $\theta_r$and $\theta_s$are the residual and saturated water content ($cm^3\ cm^{-3}$), respectively; $K_s$ is the saturated hydraulic conductivity ($cm\ d^{-1}$). The parameters $\alpha(cm^{-1})$,$n$, and $l$ are empirical coefficients affecting the shape of the hydraulic functions. The Empirical parameter $m$ is the van Genuchten model parameter which is calculated as (1 – 1/n).

The Chauka model had 201 nodes spaced at 0.005 m intervals to form a regular 1 m long grid and a surface area of 1 $m^2$. The model was divided into two layers representing the upper (0–60 cm) and the lower soil horizons (60–100 cm), based on the soil sample analysis of the trial pit in the study site (Fig. 4). HYDRUS does not calculate actual flow at the soil surface and assumes that the excess water (difference between Precipitation and Infiltration) is runoff. The land use condition like bare soil surface is represented in the form of minimum root depth. An atmospheric boundary condition with a surface layer was selected at the soil surface. The surface layer condition permits water to build upon the surface, which represents the Chauka conditions. The Chauka's are like small infiltration trenches, which are around 25–30 cm deep. The height of the surface water layer representing the ponding in the Chauka system increases due to runoff and reduces because of infiltration and evaporation. In the Chauka system, trenches of 25 cm depth were excavated in around 10% area of the total Chauka area. Since the soil moisture changes were monitored in the non-trenched area, the 25 cm depth was converted (by dividing the 25 cm depth with the non-trenched area of a chauka) to an equivalent ponding depth of $0.65 \pm 0.005$ cm over the remaining monitored area.

In this region, the average annual rainfall for the last 34 years (1971–2014) is 575.7 mm. In the year, 2019 and 2020, the total rainfall was 700 and 760 mm respectively. In the year, 2019 the highest position of the water table was at 1.79 m below ground level, however in 2020 it rose to 0.91 m below ground level, but this was in mid-September which is the last phase of monsoon in this region. We selected free drainage boundary condition based on the historical evidence that the water table in this region remains well below 1 m during the monsoon season. The Hargreaves equation (Hargreaves and Samani, 1985) was applied to compute the evapotranspiration over a reference surface, which uses the daily maximum-minimum temperature and the extraterrestrial solar radiation information. The value of global solar radiation's extinction coefficient was taken as 0.463, as suggested in the HYDRUS-1D manual (Šimůnek et al., 2008). Leaf area index values at various growth stages for the grass were obtained from the National Oceanic and Atmospheric Administration (NOAA) Climate Data Record (CDR) for 2018 and 2019 (Vermote and NOAA CDR Program, 2019). Based on the observation taken in the field using a trial pit, the value for the maximum root depth of grass in *Chauka* was taken as 50 cm (Fig. 4).

### 3.3. Soil hydraulic parameters estimation

Hydrus-1D requires the soil hydraulic parameters such as $\theta_r$, $\theta_s$, $K_s$,$\alpha$, $n$, and $l$, which can be determined using the physical properties of the soil. Soil texture is determined by the relative proportion of sand, silt, and clay. Soil samples (both disturbed and undisturbed) were collected from the catchment and Chauka site to obtain the sand, silt, and clay fractions (Gee and Or, 2002). A sieve and particle size analyser were used to determine soil texture, and the results were recorded as the percentage of sand, silt, and clay. USDA classification system was used to convert quantitative data to textural classification (Barman et al., 2019). The soil samples collected from six locations within the catchment, where the fractions of sand, slit and clay varied between 29% and 57%, 26–59% and 4–9%, respectively. The obtained soil fractions for the Chauka site were also found to be in the similar range (Table 2).

The undisturbed soil samples were used to estimate the soil bulk and dry density using the oven-dry method**.** A pressure plate experiment was done to obtain the field capacity and wilting point of the soil, which refers to moisture content corresponding to matrix suction value of 33 Kpa and 1500 Kpa, respectively. The obtained soil retention curve was fitted with the RETC model (Van Genuchten, 1980) to obtain soil retention parameters, as shown in Table 3. The saturated hydraulic conductivity was estimated using Rosetta model which uses a pedotransfer function that predicts hydraulic parameters using the soil texture data and other related information (Schaap et al., 2001). Considering the soil fractions of the Chauka site are within the range of fractions observed in the catchment, the derived parameters from the soil fractions were assumed to be representative for this small catchment.

### 3.4. Model calibration and validation

Soil parameter estimation based on field observations or laboratory analysis involves high uncertainty for most practical applications (Luo and Sophocleous, 2010). Inverse modeling has been used to estimate the soil hydraulic parameters using the time series of measured soil water content and pressure head as objective functions for parameter optimization (Jacques et al., 2002). Simulation of C*hauka* system using HYDRUS-1D with the Rosetta based hydraulic parameter resulted into recharge estimates that werein poor agreement with the observed data. Therefore, the inverse solution in HYDRUS-1D is accomplished using the Levenberg-Marquardt nonlinear minimization method (Marquardt, 1963), a standard approach for soil hydraulic parameters estimation. The water flow and root water uptake processes were selected to optimize soil hydraulic parameters using an inverse solution approach. The van Genuchten model (1980) was selected for the soil hydraulic properties, which requires calibration of some parameters such as$\theta_r$, $\theta_s$,

**Table 2**
Soil profile physical properties in *Chauka* system Lapodiya.

| Depth (cm) | Sand (%) | Silt (%) | Clay (%) | Bulk density ($g/cm^3$) | Soil type |
|---|---|---|---|---|---|
| 0–60 cm | 43 | 50 | 6.6 | 1.78 | Silt Loam |
| 60–100 cm | 53 | 41 | 5.8 | 1.89 | Sandy Loam |

**Table 3**
Soil hydraulic parameters based on RETC and Rosetta model.

| Depth (cm) | $\theta_r$ ($cm^3/cm^3$) | $\theta_s$ ($cm^3/cm^3$) | $\alpha$ (1/cm) | $n$ | $m$ | $K_s$ (cm/d) |
|---|---|---|---|---|---|---|
| 0 | 0.069 | 0.23 | 0.003 | 2.29 | 0.56 | 9.9 |
| 60 | 0.097 | 0.28 | 0.003 | 2.68 | 0.63 | 5.6 |
| Optimized parameters | | | | | | |
| 0 | 0.054 | 0.25 | 0.011 | 1.17 | 0.15 | 2.8 |
| 60 | 0.097 | 0.28 | 0.006 | 1.38 | 0.27 | 0.93 |

$K_s$,$\alpha$and $n$. The observed soil moisture data from the C*hauka* system between July and September 2019 was used for the calibration of model parameters. To identify the parameters for calibration, a sensitivity analysis was conducted. It was observed that the estimated recharge is least sensitive to the parameters such as $\theta_r$, $\theta_s$ especially in the deeper layers (60–100 cm) of the soil zone. For a $\pm$ 10% variation in $\theta_r$ and $\theta_s$, the estimated recharge varies less than 1% at 60–100 cm depth. However, the estimated recharge was found to be more sensitive to other hydraulic parameters such as $K_s$,$\alpha$ and $n$. Since Rosetta implements pedotransfer functions, which predict water retention parameters and the saturated hydraulic conductivity (Ks) based on soil data (i.e. texture class, texture distribution and bulk density), and few water retention points as input may not represent the field conditions. Therefore, most of the parameters were calibrated except the $\theta_r$ and $\theta_s$of the lower soil layer (60–100 cm).

The error between observed and simulated pressure heads in the upper and lower soil layer was minimized during parameter optimization. Though the model uses automatic optimization for the parameters, a trial and error approach was also used simultaneously to optimize the parameters systematically. A trial and error approach was also used simultaneously to ensure that the program converges to the same global minimum in the objective function. The efficacy of the calibration was checked using HYDRUS-1D model output (model fit and convergence behaviour) and visual inspection of model fitting to the field data (pressure heads). The soil moisture data of the year 2020 for the monsoon period (July-August) was used to validate the calibrated soil hydraulic parameters. During the validation process, observed and simulated pressure heads were compared. Statistical indicators such as RMSE and $R^2$ were used to assess the agreement between observed and simulated values.

### 3.5. Vegetation changes

In the ecosystems of semi-arid regions, surface processes, productivity and sustainability depend significantly on the soil moisture conditions (Porporato et al., 2002; Mishra and Singh, 2010; Legates et al., 2011; Jin et al., 2011). Soil moisture is an effective water source for plant growth in semi-arid regions (Yang et al., 2012). Its response to the changes in land cover indicates the sustainability of vegetation restoration in the region. Normalized Difference Vegetation Index (NDVI) was derived at annual scale for 1993–2019 to identify any changes in vegetation cover. NDVI is a difference between reflectance in Near-infrared (NIR) and Red spectral bands normalized by their sum. It varies between − 1 and 1, wherein the higher values reflect vegetation, and lower values indicate other classes such as bare ground and water. The NDVI has been the most widely used vegetation index to monitor vegetation coverage, health, and phenology using remote sensing images at local and global scales (Cao et al., 2018; Patidar and Keshari, 2020). In this study, a time series of Landsat images, including 418 images, was used to derive the NDVI time series. The time-series data includes images from three different Landsat sensors, including 187 images of Thematic mapper (TM), 153 images of Enhanced TM plus (ETM+), and 78 images of Operational Land Imager (OLI). The time-series analysis was performed in Google Earth Engine (Gorelick et al., 2017).

## 4. Results

Assessment of the *Chauka* system of the Lapodiya catchment is presented in this section for monsoon periods of 2019 (June-September) and 2020 (June-September). The calibration and validation results are presented for July-September (2019) and July-August (2020), respectively, as the data of soil moisture variations was available for this period only.

### 4.1. Soil properties

Table 2 shows the soil textural fractions and the bulk density of the soil profile depths of 0–60 cm and 60–100 cm in the *Chauka* system. The physical analysis indicates that the soil profile varies in texture with depth, changing from silt loam in the upper layer to sandy loam in the bottom layer. The bulk density of the soil profiles is 1.78 g $cm^{-3}$ and 1.89 g $cm^{-3}$ for 0–60 cm and 60–100 cm depth, respectively. Hunt and Gilkes (1992) suggested that the bulk density at which the root growth could be restricted varies with soil type. However, bulk densities greater than 1.6 g $cm^{-3}$ tend to restrict root growth (McKenzie et al., 2004) and indicates that soil porosity is low and soil is highly compacted. It may also cause poor movement of air and water through the soil. Initial and optimized soil hydraulic parameters of the soil profiles are provided in Table 3. The optimized $K_s$ value for 0–60 cm soil profile is higher (2.8 cm $day^{-1}$) than the 60–100 cm profile (0.93 cm $day^{-1}$) in line with the soil profiles' bulk densities. The computed Ks values are aligned with Kelishadi et al. (2014) and Kabir et al. (2020), whose models found that the soil hydraulic conductivity in semi-arid regions is less in pasturelands compared to the other cultivated soils, which García-Gutiérrez et al. (2018) attribute to high compactness due to intense animal grazing and low organic matter content. Various experimental studies have also established that if the sand is mixed with 50%

silt content in a sand-silt mixture, the average saturated hydraulic conductivity will be four orders of magnitude smaller than that of the clean sand (Bandini and Sathiskumar, 2009; Belkhatir et al., 2013).

### 4.2. Rainfall variability and depth to water level ($D_w$)

This region is known for its erratic rainfall patterns. Rainfall intensity and its distribution plays a significant role in potential recharge estimation. Fig. 5 shows the rainy days of different rainfall depth intervals for the monsoon periods of the year 2019 and 2020. According to the India Meteorological Department (IMD), a rainy day has been defined as a day with 2.5 mm or more rainfall. The recorded rainfall for the monsoon period of 2019 was 700 mm, which was distributed within 32 rainy days between July and September with four rainfall events of over 70 mm. In contrast, total rainfall of 760 mm in the monsoon season of 2020 was distributed within 36 rainy days with three large 50–60 mm events. In 2020 there were more days with rainfall between 10 and 50 mm (Fig. 5) than in 2019. Even though the total amount was lower in 2020, more days when the soil is saturated allow more infiltration to occur and reduce runoff.

The role of rainfall intensity and distribution was also evaluated by Yadav et al. under review, which suggests that the annual recharge in semi-arid regions can vary significantly due to the erratic rainfall behaviour. Despite high rainfall in 2019 or 2020, the recharge rate will be limited by the saturated hydraulic conductivity. Therefore, the above average rainfall observed in 2019 and 2020 may not necessarily recharge aquifers in these semi-arid regions due to physical limitation of aquifer parameters such as storativity and hydraulic conductivity. However, ponding in the chauka system results in decreased overland flow and provides more residence time for infiltration which will slow to a rate equal to the saturated hydraulic conductivity. Distributed rainfall events of long duration in the chauka system will lead to longer ponding times, reduced overland flow and higher recharge as long as the water table does not intersect the land surface. Therefore, in 2020, more rainfall events with low rainfall depth along with ponding over the chauka system results into more groundwater recharge. However, the impact of ponding on groundwater recharge will be limited if the heavy rains are occurring in the late monsoon season when the water table is at the ground surface high and overland flow will occur instead.

Figs. 6 and 7 show the daily rainfall, potential evapotranspiration, and corresponding change in depth to the groundwater level ($D_w$) in the *Chauka* system during the monsoon seasons of 2019 and 2020. The potential evapotranspiration varies within 2–4.5 mm/day for both the monsoon season of 2019 and 2020. The measured $D_w$ throughout the monsoon season varies within 1–5 m. In the 2019 monsoon season, the $D_w$ decreased after the frequent rainfall events in July-August and increased in late September due to pumping in the surrounding agricultural fields (Fig. 6). The trend of $D_w$ in the 2020 monsoon season is presented in Fig. 7, which shows that the early rainfall events in June have no impact on the groundwater level due to low-intensity rainfall, high evapotranspiration and high soil moisture deficit in this period. Regular rainfall events with minimum dry spells in July and August provided substantial recharge, and $D_w$ was reduced by 2.27 m (bgl) at the end of the monsoon season (Fig. 7).

### 4.3. Model calibration and validation

Simulation of field conditions using HYDRUS-1D using the hydraulic parameters obtained from the RETC and Rosetta model were in poor agreement and mismatch with the field data. Therefore, the model parameters' calibration was done using the field-based pressure head data in the objective function. Table 4 provides the goodness of fit measures for both calibration and validation stages. The coefficient of determination ($R^2$) of pressure head variation in the calibration stage for both soil profiles were 0.87 and 0.81. Further, the root mean squared error (RMSE) for pressure head data at the calibration stage was 35.66 and 26.74 cm for upper and lower soil profiles. Similarly, the $R^2$ values during the soil water content calibration stage were 0.89 and 0.87, while RMSE was 0.005 and 0.004 for the upper and lower layers. At the validation stage, the $R^2$ for pressure head data were 0.84 and 0.69, and RMSE was 40.65 and 36.63 cm for upper and lower soil profiles, respectively. Validation of soil water content in both the soil profiles was

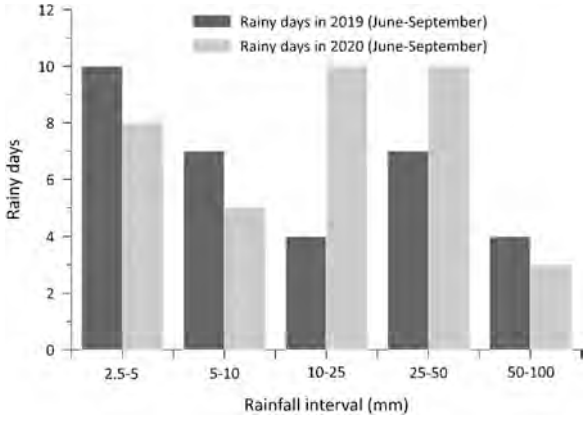


**Fig. 5.** Variation in daily rainfall depth intervals (mm) in the Lapodiya *Chauka* system during the monsoon season of 2019 (July-September) and 2020 (July-August).

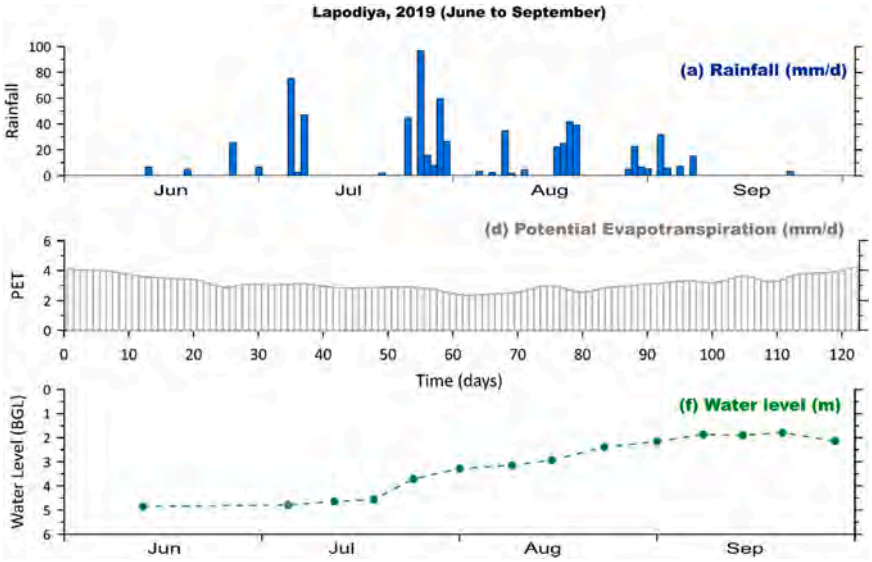


**Fig. 6.** Daily rainfall, potential evapotranspiration (PET) and depth to water level in Lapodiya catchment for the year 2019 monsoon period (June-September).

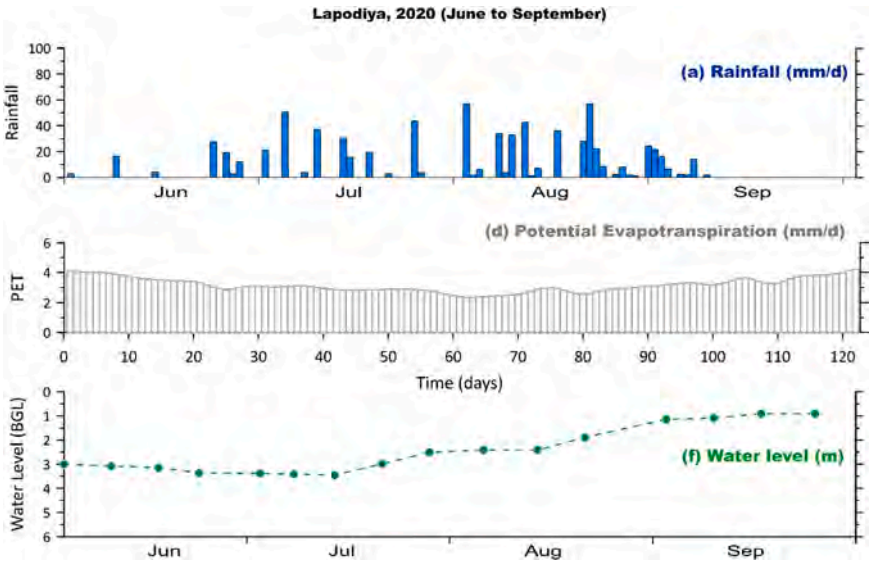


**Fig. 7.** Daily rainfall, potential evapotranspiration (PET), and depth to water level in Lapodiya catchment for the year 2020 monsoon period (June-September).

**Table 4**
The goodness of fit measures were used for simulating the pressure head and soil water content using the HYDRUS1D model in the Lapodiya catchment.

| Simulation for different soil profile depths | Dataset | Calibration | | Validation | |
|---|---|---|---|---|---|
| | | $R^2$ | RMSE (cm) | $R^2$ | RMSE (cm) |
| Surface profile (0–60) cm | Pressure head | 0.87 | 35.66 | 0.84 | 40.65 |
| | Soil water content | 0.89 | 0.005 | 0.85 | 0.006 |
| Deeper profile (60–100) cm | Pressure head | 0.81 | 26.74 | 0.69 | 36.63 |
| | Soil water content | 0.87 | 0.004 | 0.76 | 0.005 |

found acceptable, as the $R^2$ was 0.85 and 0.76 and RMSE was 0.006 and 0.005. Though the variability in the pressure head was higher, in our case, the calibration and validation performance was acceptable for most cases.

With the fitted parameterization, Hydrus-1D was then used to forecast the root zone soil moisture dynamics for pastureland during the monsoon season of 2019 and 2020. Figs. 8 and 9 show the variation in pressure head and soil water content for two depths (0–60 and 60–100) in the soil profile with the fitted parameters (Hydrus 1D) at the calibration and validation stage, respectively. The above-mentioned figures give a visual comparison of overall model performance during the calibration and validation stages. The high $R^2$values for both soil profile depths for pressure head show the agreement between the field-measured and Hydrus simulated results. A similar trend was observed with RMSE values for both the depths. Thus, HYDRUS 1D performance for soil water content simulation was good for both calibration and validation stages; however, the modeling performance of the pressure head for the validation dataset shows moderate performance compared to the calibration dataset.

### 4.4. Water balance and groundwater recharge

This *Chauka* system is used as pastureland in the monsoon season and provides a significant opportunity for groundwater recharge. The calibrated model of the *Chauka* system was used to estimate the potential groundwater recharge during the monsoon period of the years 2019 and 2020. Since the area is barren land, excess runoff of the rainfall (*P*) was the only input component. Evaporation *(E)*, runoff ($Q_r$), water uptake by the natural grassroots (*T*), drainage below the soil zone ($R_e$), and soil water storage change (*dv*) in the root zone were considered as the output components. Excess water drained below the soil zone was considered as the potential groundwater recharge. An approximate ponding depth of 6.5 mm was considered to estimate the potential recharge for the monsoon period of 2019 and 2020.

The water balance obtained from the calibrated and validated HYDRUS-1D model of the *Chauka* system (0 and 6.5 mm ponding) for the monsoon period in 2019 and 2020 is presented in Table 5. Evapotranspiration (evaporation and root water uptake) for both years was 238 mm and 267 mm when 6.5 mm ponding was allowed in the *Chauka* system. Evapotranspiration *(ET)* increases with increasing seasonal water input, which in this case, includes excess runoff only. The average evapotranspiration rate for the 2019 and 2020 monsoon periods was 1.95 mm/day and 2.18 mm/day, respectively. The water availability for *ET* was higher in the monsoon period of 2020, resulting in higher *ET*. The *ET* rate also increases with the decrease in depth to the groundwater level, and therefore reduced depth to the water level in 2020 could have enhanced the average *ET* rate (Fig. 11).

The evaporation is higher in case of ponding during 2020. However, In 2019, the evaporation was equal between zero ponding and 6.5 mm ponding scenarios. Low evaporation during the 6.5 ponding case might result from skewed rainfall distribution, which is concentrated within a few days with many dry spells. Also, the higher runoff in the year 2019 resulted from high-intensity rainfall events distributed in a short period. It is evident from Figs. 6 and 7 that the high-intensity rainfall is concentrated in a few days and there are many dry spells in the 2019 monsoon season; but in 2020 rain is well distributed across July and August. Further, such low evaporation in the year 2019 might be the HYDRUS atmospheric boundary condition which allows water to evaporate from the soil surface at the potential rate as long as the pressure head at the surface remains above a threshold value. If the soil surface dries out such that the surface pressure head reaches the threshold value, the boundary switches to a constant pressure head condition, generally leading to a computed actual evaporation rate that is well below the potential rate.

In combination with high rainfall intensity and low evapotranspiration, the bareness of the land and moderate slopes cause

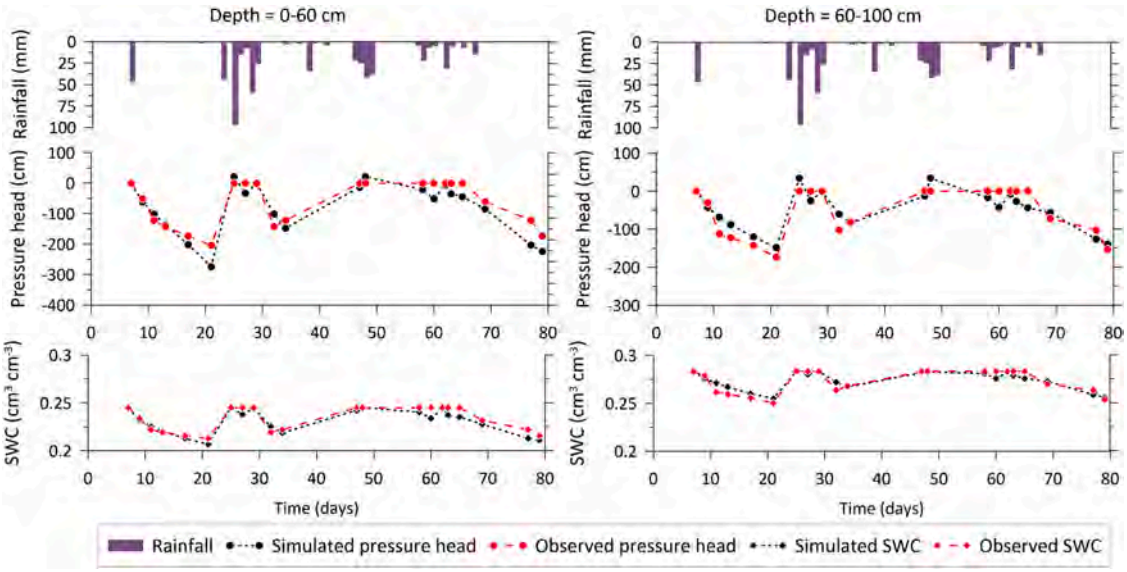


**Fig. 8.** Calibration of the HYDRUS 1D model for the field conditions of Lapodiya catchment during the monsoon period of 2019 (July-September).

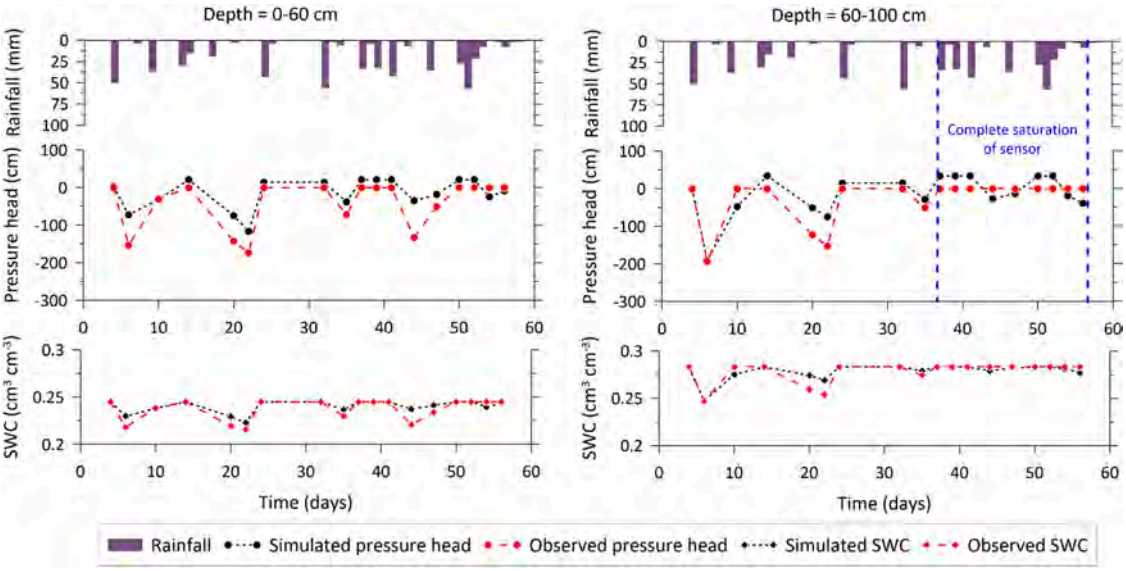


**Fig. 9.** Validation of the HYDRUS 1D model for the field conditions of Lapodiya catchment during the monsoon period of 2020 (July-August).

**Table 5**
Soil water balance of the *Chauka* system in the monsoon period of 2019 (July-September) and 2020 (July-September), considering different ponding depths.

| Water Balance Components | 2019 | | 2020 | |
|---|---|---|---|---|
| | Ponding depth (mm) | | Ponding depth (mm) | |
| | 0 | 6.5 | 0 | 6.5 |
| Rainfall ($P$), mm | 700 | 700 | 760 | 760 |
| Evaporation ($E$), mm | 151 | 151 | 183 | 187 |
| Root water uptake ($T$), mm | 90 | 87 | 90 | 80 |
| Potential Recharge ($R_e$) mm | 187 | 222 | 177 | 258 |
| Runoff ($Q_r$), mm | 314 | 259 | 240 | 180 |
| Water balance ($P$-$E$-$R_e$-$Q_r$-$T$), mm | -41 | -20 | 70 | 55 |
| Change in storage ($dv$), mm | -17 | -17. | 72 | 73 |
| Absolute error (%) | *3.40* | *0.37* | *0.26* | *2.33* |

significant surface runoff in these areas. As presented in Table 5, in the monsoon period of 2019, approximately 37% of total rainfall is lost through runoff, while it was 23% for the 2020 monsoon period. The higher runoff in the year 2019 resulted from high-intensity rainfall events distributed in a short period. It is evident from Figs. 6 and 7 that the high-intensity rainfall is concentrated in few days with many dry spells in the 2019 monsoon season; however, it is well distributed between the July and August months of 2020.

In the monsoon season of 2019, the total potential groundwater recharge was 222 mm, about 31.8% of the total rainfall of 700 mm (Table 5). Potential groundwater recharge was also estimated for the monsoon season of 2020, which was 258 mm, approximately 34% of the total rainfall of 760 mm in this period. Change in the soil water storage in this region can be attributed to recharge and evapotranspiration from groundwater. In the monsoon period of 2019, the change in storage was negative (Table 5) due to a lack of rainfall and a high evapotranspiration rate in September. However, the change in soil water storage during the monsoon period of the year 2020 was positive, as recharge is the dominating factor at this stage. Table 5 also presents the absolute error in the water balance for both the 2019 and 2020 monsoon periods, which is less than 3% for both the years.

Table 5 also presents the scenarios with zero ponding depth to highlight the importance of the *Chauka* system in barren lands. The depth of ponding on the *Chauka* surface increases due to excess runoff and reduces because of infiltration and evaporation. In 2019, 6.5 mm of ponding increased the potential amount of recharge from 187 mm (no ponding) to 222 mm. The impact of such an increase could also be seen in the reduction of runoff amount from 314 mm to 259 mm. Similarly, in the 2020 monsoon period, the estimated potential recharge increased from 177 mm in with no ponding case to 258 mm for 6.5 mm ponding. Reduction in the runoff from 240 mm to 180 mm was also observed when 6.5 mm ponding was allowed on the *Chauka* system surface. The comparative analysis of zero ponding and 6.5 mm of ponding on the *Chauka* system indicates that the small storage rainwater harvesting structures like *Chauka* have the potential to provide substantial groundwater recharge.

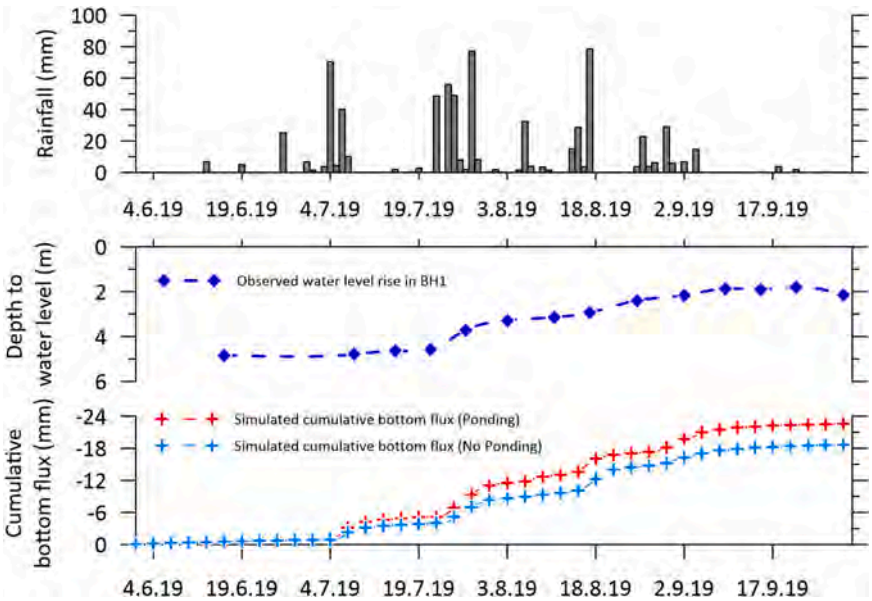


**Fig. 10.** Observed depth to water level ($D_w$) rise in the borehole BH1 located in the *Chauka* system along with the increase in cumulative bottom flux (recharge) in both ponding and no ponding scenarios resulting from the rainfall in the monsoon period of 2019.

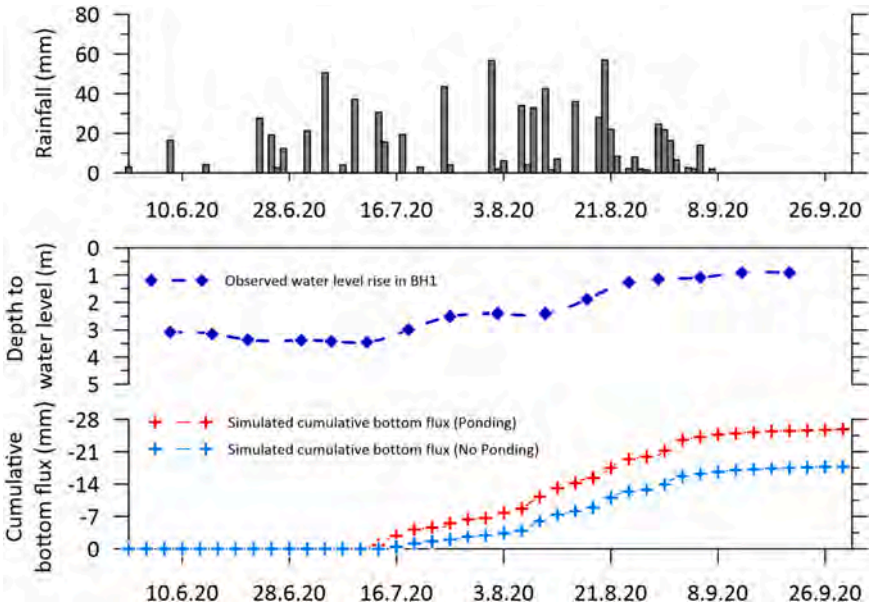


**Fig. 11.** Observed depth to water level ($D_w$) rise in the borehole (BH1) located in the *Chauka* system along with the increase in cumulative bottom flux (recharge) in both ponding and no ponding scenarios resulting from the rainfall-runoff in the monsoon period of 2020.

### *4.5. Water table response*

A borehole was installed and monitored weekly since June 2019 to monitor the water table response due to recharge from the *Chauka* system (BH1). Groundwater is extracted from large diameter wells using diesel pumps operating extensively for irrigation during the winter, resulting in the decline of the groundwater table. As shown in Fig. 10 that the depth to water level was 4.85 m bgl in mid-June 2019 (16th June) and rose up to 2.14 m bgl by the end of September (29th September). The total rise in the depth to the water level in this period was 2.71 m with an average rate of 26 mm/day. The obtained cumulative bottom flux (potential groundwater recharge) from the developed model was also mapped with the depth to water level rise in BH1 (Fig. 10), suggesting that the estimated potential recharge is acceptable. The cumulative bottom flux of ponding and no ponding scenarios in Fig. 10 indicates that the ponding

over the *Chauka* surface provides additional groundwater recharge in the monsoon period of 2019.

Fig. 11 shows the water table rises in BH1 during the monsoon season of the year 2020, along with the increase in cumulative bottom flux (potential groundwater recharge) for ponding and no ponding situations of the *Chauka* system, which follow a similar rising trend supporting the suitability of the approach adopted. In this period, the water table rose from 3.41 m bgl in early July (5th July) to 0.91 m bgl at the end of September (20th September) 2020. In this period, the depth to water level rose up to 2.5 m with an average rate of 28 mm/day. The rate of rise in the water table in different years could be due to the variability in the amount and intensity of rainfall in the local area. A further limitation is the possible impact of the river and other ponds on recharge in the area. The river only flows for a short period after rains. The other ponds are designed for storage and are constructed on impermeable soil types. The borehole is within the chaukas so they will be having the biggest impact, but it is hard to separate them.

Groundwater occurrence in these low porosity hard-rock areas is found in the weathered and fractured zones that primarily govern groundwater storage and transmission in these rocks. A constant specific yield of 0.1 was used based on the studies conducted in similar lithological formations of Rajasthan state (COMMAN, 2005; Glendenning and Vervoort, 2010). By taking the potential recharge value of 222 mm and a constant $S_y$ of 0.1, the water level in the 2019 monsoon period rose by up to 2.22 m ($Re/S_y$). Similarly, in the monsoon period of 2020, the rise in the water table from the potential recharge of 258.44 mm was 2.58 m. The specific yield-based rise in the water table of 2.22 m is 18% less than the actual rise of 2.71 m in 2019. However, in the monsoon period of 2020, it is 3.2% higher than the 2.5 m actual rise. It is important to note here that the spatial variation in the specific yield can be very significant due to heterogeneity and anisotropy in aquifer properties that are characteristic of hard rock aquifers. The specific yield of hard rock aquifer also varies with the depth due to change in fracture density and porosity with depth (Maréchal et al., 2004; Dewandel et al., 2006). Therefore, a sensitivity analysis was performed to identify the optimum value of Sy for the Lapodiya sub-catchment. The Sy values ranging from 0.01 to 0.15 were used to convert the estimated potential recharge into the water level rise in the aquifer. The analysis suggests that a Sy value of 0.1 produces minimum error between the estimated water level rise and observed water level rise in BH1 for the 2019 and 2020 monsoon periods.

### 4.6. Impact on vegetation

The change in vegetation cover of this area can be seen in Fig. 12, which compares chauka and non-chauka sites using the NDVI time series from 1993 to 2019. It is evident that the chauka area has better vegetation coverage/health. We hypothesize that the chaukas increase the soil moisture available to plants in a long-term way that makes the plants resilient to withstand short-term precipitation deficits. High precipitation years, including 1996 and 2010–12, reflect higher NDVIs; however, the NDVI has increased every year despite significant fluctuations in precipitation. Despite various changes in precipitation, the NDVI of the chauka

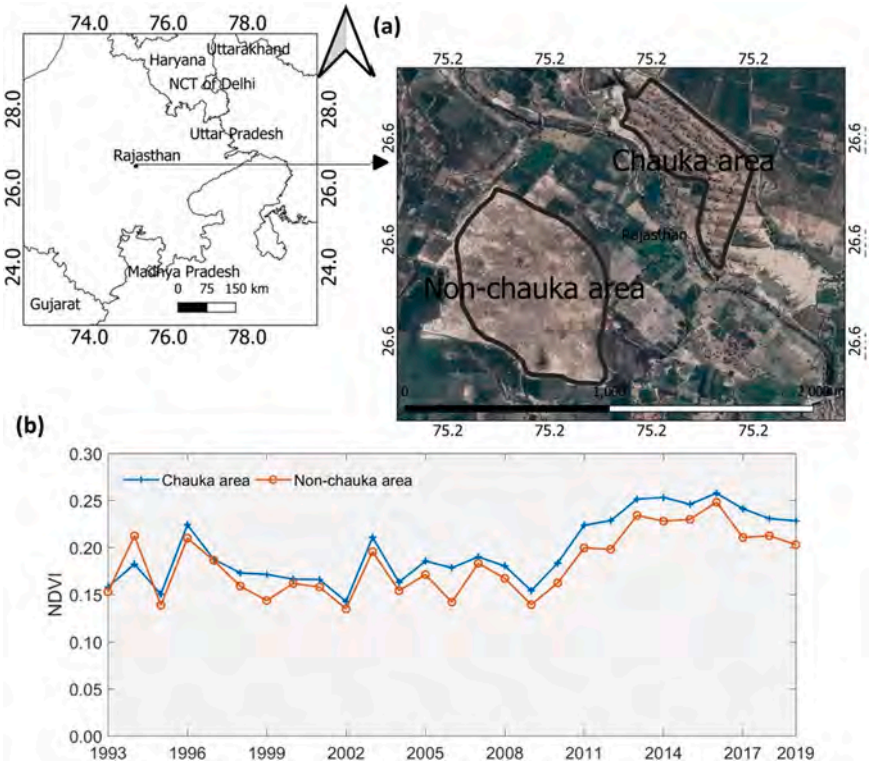


**Fig. 12.** Location of *Chauka* and non- *Chauka* areas (panels (a)), and NDVI from 1993 to 2019 in *Chauka* and non- *Chauka* areas (panel (b)).

area remains consistently higher than the non-chauka area throughout the period from 1993 to 2019. Very similar results were obtained in a recent study by Everard and West (2021) between 2016 and 2019 using the Modified Mann-Kendall test (Hamed and Rao, 1998; Hussain and Mahmud, 2019). It is demonstrated that NDVI values increase every year (a significant positive trend with a p-value of 0.008). On the contrary, there is no correlation between NVDI values and precipitation, and the trend in precipitation from 1993 to 2019 is found to be insignificant (p-value of 0.802) (Fig. 13). The rise in NDVI values, especially after 2009, could be attributed to the plantation.

In the year 1981, the area was completely barren. The renovation and augmentation of water resources started in this area in the early 1980 s. The people of nearby villages decided to conserve rainwater and soil moisture, which led to the innovation of the Chauka system. Unfortunately, NVDI data is not available before 1993, which is a limitation of this analysis. We also only have the GVNML's accounts that the chauka building has been the only activity, and there have been no other land management interventions. In the present conditions, the Chauka system serves Lapodiya village's needs by providing assured pastureland in the early dry periods. Further, investigations are suggested to understand the role of the Chauka system in ecological sustainability and land cover improvements.

### 4.7. Sensitivity analysis

The modeling approach used in this study has potential sources of uncertainty in parameters such as soil hydraulic parameters, evapotranspiration rates, crop parameters, and root water uptake parameters. This study has limited scope to consider the quantifying uncertainty in the crop parameters and root water uptake parameters. However, the uncertainly in the soil hydraulic parameters could be addressed based on the confidence intervals obtained from HYDRUS and Rosetta models. Since the parameters obtained from Rosetta models are just based on the soil properties, the estimates are significantly broad in the range. However, a sensitivity analysis was performed to understand the impact of parametric uncertainty on the estimated potential recharge. In this analysis, the model parameters such as $\theta_r$ $\theta_s$ $\alpha$, $n$ and $K_s$were perturbated a fixed amount keeping all other parameters at a baseline value. The parameters were varied separately for upper and lower soil layers. Parameter uncertainty was performed by perturbing each soil hydraulic parameter by $\pm$ 10% increment up to $\pm$ 40% from the optimized values (Table 3). Fig. 14 shows the parameter sensitivity analysis at the top (0−60) cm and bottom (60−100) cm soil depths that explains the relative importance of soil hydraulic parameters in

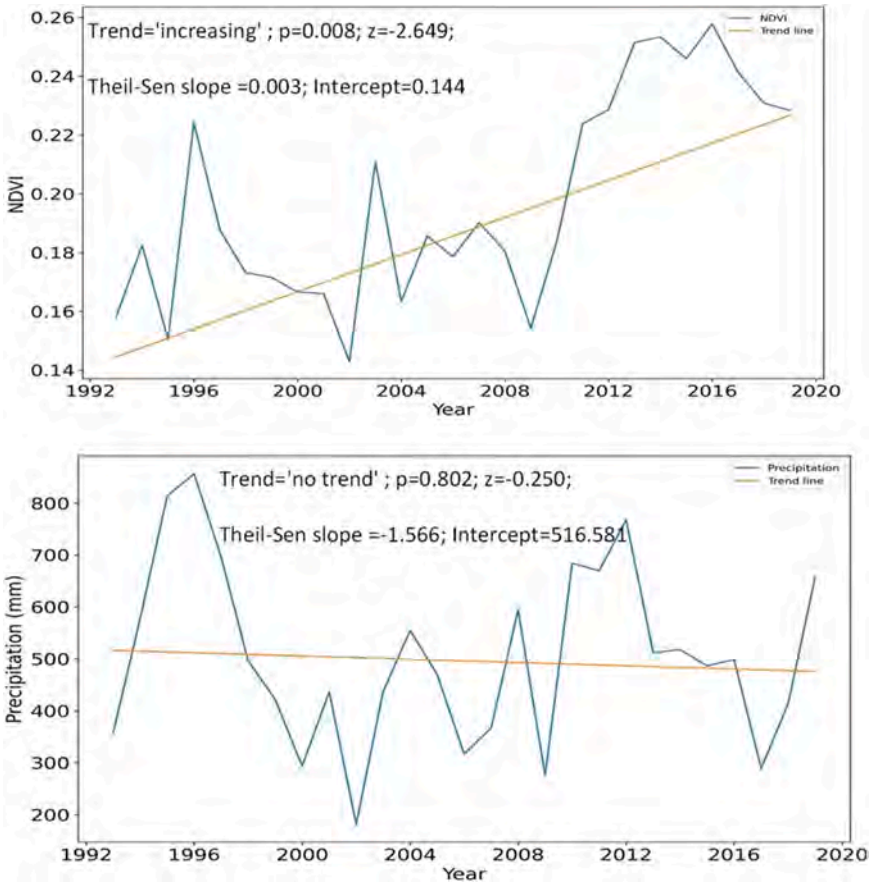


**Fig. 13.** Trend in NDVI and annual precipitation in the study area.

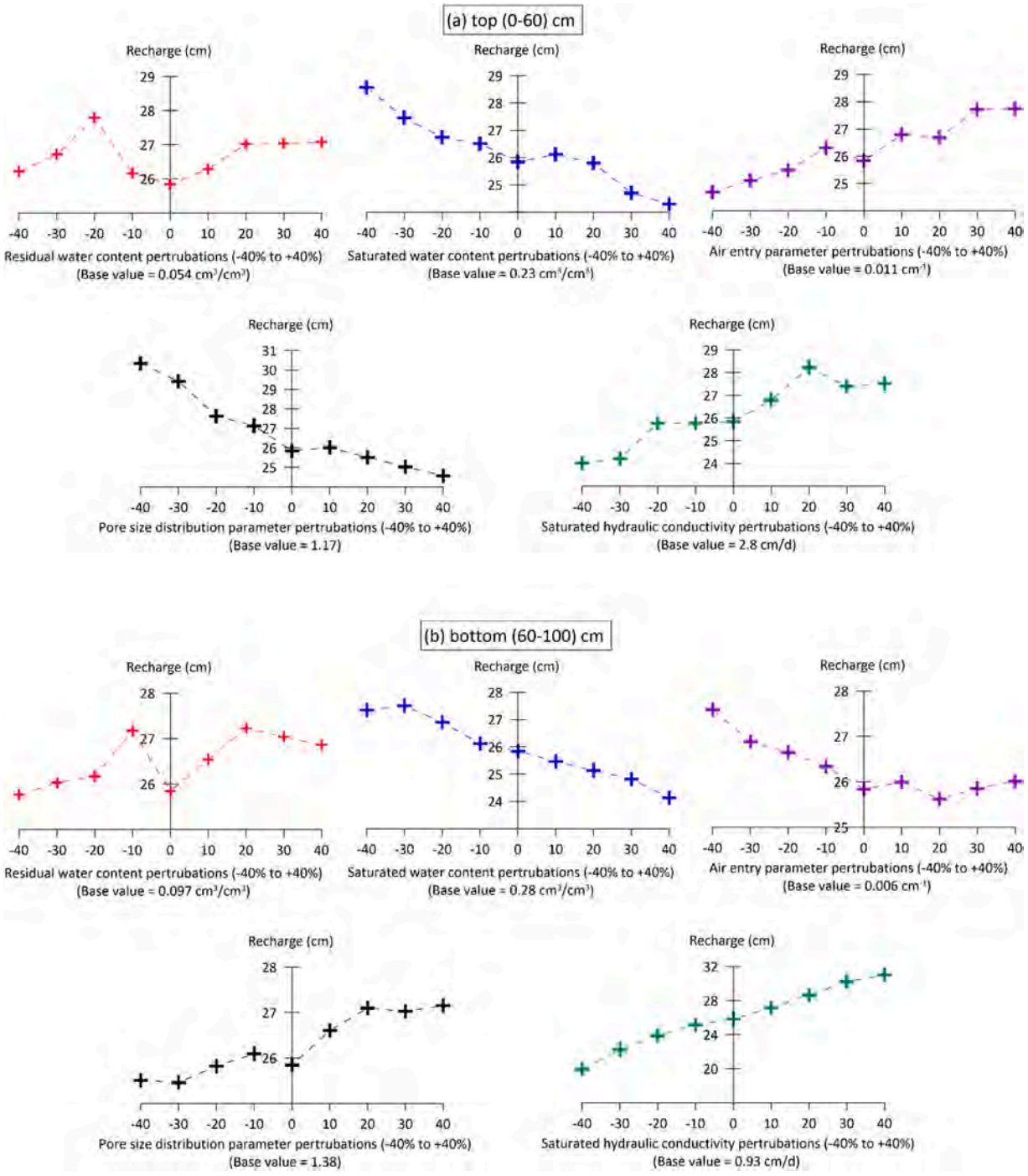


**Fig. 14.** Sensitivity analysis of soil hydraulic parameters in (a) top (0−60) cm and (b) bottom (60−100) cm soil depths. An increment of ± 10% perturbs the parameters up to ± 40% from the optimized soil hydraulic parameters.

quantifying recharge (cm). The sensitivity of soil hydraulic parameters is different in the top (0−60) cm and bottom (60−100) soil depths. In the topsoil, n is the most sensitive parameter, followed by $K_s$ and $\theta_r$. While in the bottom soil zone, $K_s$ is the most sensitive parameter to affect recharge, followed by $\theta_s$. This shows that $K_s$ is the critical parameter that affects the recharge significantly for the two soil profiles.

## 5. Discussion

The water balance in the *Chauka* system for the monsoon season of 2019 and 2020 suggests that the *Chauka* system's additional storage provides more water for potential groundwater recharge (Table 5). This is further confirmed by the comparative analysis of zero ponding and a 6.5 mm ponding scenario over the *Chauka* surface, which suggested that the additional ponded water on the *Chauka* surface reduces runoff significantly in 2019 and 2020 monsoon seasons. The average daily water table rise of BH1 in 2020 was higher (29 mm/day) than in 2019, as the larger number of rainy days permitted more recharge, even though the total rainfall was less in 2020 (Fig. 5). The recovery of well water level in the *Chauka* system also reflected a similar pattern found in the cumulative potential recharge in both the 2019 and 2020 monsoon seasons (Figs. 10 and 11).

The groundwater level rise in BH1 due to the recharge was estimated using a constant specific yield. Data on aquifer parameters such as hydraulic conductivity and specific yield is scarce in India (Chinnasamy and Agoramoorthy, 2015). In this case, a specific yield of 0.1 was used based on the studies conducted in similar lithological formations of Rajasthan state (COMMAN, 2005; Glendenning and Vervoort, 2010). The difference between the observed groundwater level rise and estimated groundwater level rise based on the specific yield was 18% in 2019 and 3.2% in the 2020 monsoon periods. Specific yield affects the accuracy and confidence level of the recharge rate (Kim et al., 2010). Other potential sources of uncertainty include soil hydraulic parameters, the daily reference evapotranspiration rate, rainfall, and root water uptake parameters (Jiménez-Martínez et al., 2009). In the case of soil hydraulic parameters, the calibration and validation results are presented with the correlation coefficients computed by HYDRUS-1D as part of the parameter optimization. Further, the range of soil hydraulic parameters was obtained from the Rosetta model using the soil texture and bulk density information. Spatial variability of the soil moisture in the catchment could also result in uncertain recharge estimations. However, it has been found in various studies that the spatial variability in the soil moisture was higher in dry periods as compared to the wet periods (Zucco et al., 2014; Dari et al., 2019). Therefore, just one sensor-based soil moisture monitoring may be sufficient to represent the catchment behavior in wet periods (i.e., monsoon), especially in the smaller catchments.

The key parameters which might have impacted the recharge estimates are $K_s$ and n, while the other parameters will have little impact on results. Since the direct measurement of recharge flux was not available, we used the observed groundwater head for calibration/validation. Recharge is converted to groundwater head by dividing it with the specific yield (recharge/sp.yield). Therefore, the uncertainty in specific yield might have propagated to the estimated rise in groundwater head. However, when used in terms of bottom flux, the recharge is free from the uncertainty in specific yield as it was not used in HYDRUS.The average annual rainfall in the study area for the last 34 years is 575.7 mm with the average annual pan evaporation of 1744.7 mm (CGWB, 2017). The vegetation growth in the semi-arid regions is generally restricted due to the low soil moisture availability. Such low soil moisture conditions are commonly observed in the semi-arid regions where the low precipitation and high evaporation combination leaves insufficient soil moisture content (Yang et al., 2012). Landscape management, such as micro-topography reconstruction, can effectively increase rainwater infiltration (Previati et al., 2010; Rejani and Yadukumar, 2010). The NDVI time-series analysis in the Lapodiya region from 1993 to 2019 indicates that the vegetation growth has increasded (Fig. 12). However, a detailed investigation of soil moisture dynamics and its relations to vegetation growth and sustainability in different seasons and the effects of landscape management on soil moisture dynamics is recommended for future research. This study was performed on a small field site with soil moisture and water level recorded at a single location, and hence it is limited to one-dimensional analysis. However, the local impact of these small-scale rainwater harvesting structures on the amount of recharge is clearly demonstrated in this study. Future studies could consider the spatial variability in the recharge potential of these systems using more detailed data at both spatial and temporal scales.

There have been various studies to estimate groundwater recharge in the northwest of India. Rangarajan and Athavale (2000) used the tritium injection method in a rainfed grassland setting in 1972–1973 and 1994–1995. They reported the median recharge rates of 35, 43, and 67 mm/year, representing 8%, 9%, and 14% of rainfall (460, 470, and 491 mm), respectively. Scanlon et al. (2010a), (2010b) studied the recharge potential of a rain-fed/irrigated cropland using the Cl mass balance approach and nutrient availability method and found a similar recharge rate of 61–94 mm/year (10–16% of precipitation, 600 mm/year) for rain-fed agriculture in a study area in Jaipur. Both of these studies were in areas where no MAR structures were present. Further, such low recharge values may also result from variable rainfall intensity and uneven distribution. Yadav et al. (under review) indicated that in semi-arid regions, a substantial amount of rainfall is required to reduce a high soil moisture deficit and increase the moisture content of the soil to its field capacity. Further, rainfall variability in semi-arid regions is also a significant factor in groundwater recharge. Conversely, Glendenning and Vervoort (2010) made field observations in the Arvari River catchment of Rajasthan, where check dams and ponds had been

**Table 6**
Approximate potential recharge contribution from the *Chauka* system as a percentage of rainfall in the monsoon seasons of 2019 and 2020.

| *Chauka* system | 2019 | | 2020 | |
|---|---|---|---|---|
| | Ponding depth (mm) | | Ponding depth (mm) | |
| | 0 | 6.5 | 0 | 6.5 |
| Rainfall ($P$), mm | 700 | 700 | 760 | 760 |
| Potential Recharge ($_{Re}$) mm | 187 | 222 | 177 | 258 |
| Recharge from *Chauka* system (%) | *5.1%* | | *4.9%* | |

Recharge from Chauka system (%) $= [(R_{e(6.5)} - R_{e(0)})/p] \times 100$

constructed to recharge groundwater. They calculated the potential recharge in the range of 200–300 mm, which is close to the results reported in this study.

The *Chauka* system caused an additional 5.1% and 4.9% of the total rainfall to become groundwater recharge during the monsoon season of 2019 and 2020, respectively (Table 6). This is again similar to Glendenning and Vervoort (2010), who found that check dams and ponds contributed an additional 6–7% of recharge, and also Sharda et al. (2006) and Badiger et al. (2002), who studied various MAR structures and found that up to 10% of rainfall becomes potential recharge. The significant contribution of these *Chauka* systems in intercepting the runoff and allowing it to infiltrate into the ground surface provides a promising small-scale solution for water scarcity in the semi-arid regions. The ability of *Chauka* systems to intercept runoff and provide additional recharge is reflected in Table 6, which indicates that the recharge in 2019 and 2020 increased by 19% and 46%, respectively, relative to the recharge when no ponding is allowed on the surface. Such high interception of runoff is extremely important for this region which has significant variability in the rainfall both at spatial and temporal scales. This analysis also indicates that the groundwater recharge in this area is dependent on rainfall attributes (intensity and distribution) which determines the rate and pattern of the water balance components and hence the groundwater resources. The evidence presented here suggests they effectively increase both recharge and vegetation and should be considered for implementation more widely. Furthermore, this study suggests few geographical constraints to their application, if there is slightly sloping, barren land above an unconfined aquifer, this approach could be tried. This study also highlights the potential value in traditional rainwater harvesting systems to restore the depleted shallow groundwater aquifers. It should be added to those documented elsewhere (for example, Sharma et al, 2018). Traditional approaches are well adapted to local demand, culture, and hydro-geography.

## 6. Conclusion

Small-scale rainwater harvesting using both traditional and modern rainwater harvesting structures is being implemented in India to alleviate declining groundwater stores, but there is a need for a better understanding of the impacts of many small rainwater harvesting structures and their broader role in water resources management. Field data was collected during this study in the monsoon periods of 2019 and 2020. There were many challenges working in a resource-poor setting and the field data set is not fully comprehensive, but nevertheless the study has highlighted the importance of these traditional structures in semi-arid regions. The *Chauka* system transforms approximately 5% rainfall runoff to recharge in both the 2019 and 2020 monsoon seasons. Further, the vegetation index derived from satellite data also highlights the contribution of the *Chauka* system in altering the near soil surface moisture, which helps develop pasturelands used in early dry periods, although this conclusion comes with the caveat that the chaukas were constructed prior to the availability of satellite data.

## CRediT authorship contribution statement

**Basant Yadav**: Conceptualization, Data collection, Data curation, Methodology, Formal analysis, Writing – original draft. **Nitesh Patidar:** Formal analysis, Writing – review & editing. **Anupma Sharma**: Conceptualization, Funding acquisition, Supervision, Writing – review & editing. **Niranjan Panigrahi**: Formal analysis, Writing – review & editing. **Rakesh Sharma**: Writing – review & editing. **V Loganathan**: Writing – review & editing. **Gopal Krishan**: Writing – review & editing. **Suraj Kumar**: Data collection and analysis. **Jaswant Singh**: Data collection and analysis. **Alison Parker**: Conceptualization, Funding acquisition, Methodology, Supervision, Writing – review & editing.

## Declaration of Competing Interest

The authors declare that they have no known competing financial interests or personal relationships that could have appeared to influence the work reported in this paper.

## Data Availability

Data underlying this paper can be accessed at: https://10.17862/cranfield.rd.13348424.

## Acknowledgments

The research was funded by NERC-DST (Grant Ref: NE/R003351/1). The authors would like to thank Prof. Ken Rushton for the valuable insights on recharge estimation. The following people are thanked for their support during the fieldwork: Mr. Jagveer Singh, Sangram Singh, Sanju Devi.

## Appendix A. Supporting information

Supplementary data associated with this article can be found in the online version at doi:10.1016/j.ejrh.2022.101149. These data include Google maps of the most important areas described in this article.

## References


Badiger, S., Sakthivadivel, R., Aloysius, N., Sally, D. (2002). Preliminary assessment of a traditional approach to rainwater harvesting and artificial recharging of groundwater in Alwar District, Rajasthan. In: Annual Partners'Meet2002, IWMI- TATA Water Policy Research Program, pp. 1–18.

Bandini, P., Sathiskumar, S., 2009. Effects of silt content and void ratio on the saturated hydraulic conductivity and compressibility of sand-silt mixtures. J. Geotech. Geoenviron. Eng. 135 (12), 1976–1980.

Belkhatir, M., Schanz, T., Arab, A., 2013. Effect of fines content and void ratio on the saturated hydraulic conductivity and undrained shear strength of sand–silt mixtures. Environ. Earth Sci. 70 (6), 2469–2479.

Cao, R., Chen, Y., Shen, M., Chen, J., Zhou, J., Wang, C., Yang, W., 2018. A simple method to improve the quality of NDVI time-series data by integrating spatiotemporal information with the Savitzky-Golay filter. Remote Sens. Environ. 217, 244–257.

Central Ground Water Board (CGWB), 2012. Aquifer systems of India. Government of India, Ministry of Water Resources, New Delhi, India. ⟨http://cgwb.gov.in/AQM/India.pdf⟩.

Central Ground Water Board (CGWB), 2013. Ground Water Information Jaipur District Rajasthan. Government Of India Ministry Of Water Resources Central Ground Water Board, Jaipur.

Central Ground Water Board (CGWB). (2015). Ground Water Year Book, 2015–16. Ministry of Water Resources, New Delhi, India.

Central Ground Water Board (CGWB), 2017. Aquifer Mapping And Ground Water Management - Jaipur District, Rajasthan, Jaipur. Ministry of Water Resources, River Development and Ganga Rejuvenation - Government of India,. http://cgwb.gov.in/AQM/NAQUIM_REPORT/Rajasthan/Jaipur.pdf.

Chinnasamy, P., Agoramoorthy, G., 2015. Groundwater storage and depletion trends in Tamil Nadu State, India. Water Resour. Manag. 29 (7), 2139–2152.

COMMAN, (2005). Community management of groundwater resources in Rural India: background papers on the causes, symptoms and mitigation of ground- water overdraft in India. British Geological Survey Commissioned Report CR/05/36N.

Coyte, R.M., Jain, R.C., Srivastava, S.K., Sharma, K.C., Khalil, A., Ma, L., Vengosh, A., 2018. Large-scale uranium contamination of groundwater resources in India. Environ. Sci. Technol. Lett. 5 (6), 341–347.

Dari, J., Morbidelli, R., Saltalippi, C., Massari, C., Brocca, L., 2019. Spatial-temporal variability of soil moisture: addressing the monitoring at the catchment scale. J. Hydrol. 570, 436–444.

Dewandel, B., Lachassagne, P., Wyns, R., Maréchal, J.C., Krishnamurthy, N.S., 2006. A generalized 3-D geological and hydrogeological conceptual model of granite aquifers controlled by single or multiphase weathering. J. Hydrol. 330 (1–2), 260–284.

Everard, M., West, H., 2021. Livelihood security enhancement though innovative water management in dryland India. Water Int. 46 (1), 59–82 (sss).

Feddes, R.A., Kowalik, P., Zarandy, H., 1978. Simulation of field water use and crop yield. Pudoc. Wageningen. The Netherlands saline water in supplemental irrigation of wheat and barley under rainfed agriculture. Agric. Water Manag. 78, 122–127.

Food and Agriculture Organization. (2016). AQUASTAT Main Database. Available at: ⟨http://www.fao.org/nr/water/aquastat/data/query/index.html?lang=en⟩ (Accessed: 31 May 2018).

García-Gutiérrez, C., Pachepsky, Y., Martín, M.Á., 2018. Saturated hydraulic conductivity and textural heterogeneity of soils. Hydrol. Earth Syst. Sci. 22 (7), 3923–3932.

Gee, G.W., Or, D., 2002. 2.4 Particle-size analysis. Methods of soil analysis. Part 4 (598), 255–293.

Glendenning, C.J., Vervoort, R.W., 2010. Hydrological impacts of rainwater harvesting (RWH) in a case study catchment: the Arvari River, Rajasthan, India. Part 1: field-scale impacts. Agric. Water Manag. 98 (2), 331–342.

Gontia, N.K., Sikarwar, R.S., 2005. Rainwater harvesting and groundwater recharge in Saurashtra region of Gujarat—a success story. Indian J. Soil Conserv. 33 (3), 256–258.

Gorelick, N., Hancher, M., Dixon, M., Ilyushchenko, S., Thau, D., Moore, R., 2017. Google Earth Engine: planetary-scale geospatial analysis for everyone. Remote Sens. Environ. 202, 18–27.

Gram Vikas Navyuvak Mandal Lapodiya, 2007. The Chauka System: Innovation in Soil and Water Conservation. UNICEF, Jaipur.

Hamed, K.H., Rao, A.R., 1998. A modified Mann-Kendall trend test for autocorrelated data. J. Hydrol. 204 (1–4), 182–196. https://doi.org/10.1016/S0022-1694(97)00125-X.

Hargreaves, G.H., Samani, Z.A., 1985. Reference crop evapotranspiration from temperature. Appl. Eng. Agric. 1 (2), 96–99.

Hunt, N., Gilkes, R., 1992. Farm Monitoring Handbook–A Practical Down-toearth Manual for Farmers and Other Land Users. University of Western Australia: Nedlands, WA, and Land Management Society, Como, WA.

Hussain, M.M., Mahmud, I., 2019. pyMannKendall: a python package for non parametric Mann Kendall family of trend tests. J. Open Source Softw. 4 (39), 1556. https://doi.org/10.21105/joss.01556.

Jacques, D., Šimůnek, J., Timmerman, A., Feyen, J., 2002. Calibration of Richards' and convection–dispersion equations to field-scale water flow and solute transport under rainfall conditions. J. Hydrol. 259 (1–4), 15–31.

Jiménez-Martínez, J., Skaggs, T.H., Van Genuchten, M.T., Candela, L., 2009. A root zone modelling approach to estimating groundwater recharge from irrigated areas. J. Hydrol. 367 (1–2), 138–149.

Jin, T.T., Fu, B.J., Liu, G.H., Wang, Z., 2011. Hydrologic feasibility of artificial forestation in the semi-arid Loess Plateau of China. Hydrol. Earth Syst. Sci. 15, 8.

Kabir, E.B., Bashari, H., Bassiri, M., Mosaddeghi, M.R., 2020. Effects of land-use/cover change on soil hydraulic properties and pore characteristics in a semi-arid region of central Iran. Soil Tillage Res. 197, 104478.

Kelishadi, H., Mosaddeghi, M.R., Hajabbasi, M.A., Ayoubi, S., 2014. Near-saturated soil hydraulic properties as influenced by land use management systems in Koohrang region of central Zagros, Iran. Geoderma 213, 426–434.

Kim, G.B., Choi, D.H., Jeong, J.H., 2010. Considerations on the specific yield estimation using the relationship between rainfall and groundwater level variations. J. Eng. Geol. 20 (1), 61–70.

Kumar, M.D., Patel, A., Ravindranath, R., Singh, O.P., 2008. Chasing a mirage: water harvesting and artificial recharge in naturally water-scarce regions. Econ. Political Wkly. 61–71.

Legates, D.R., Mahmood, R., Levia, D.F., DeLiberty, T.L., Quiring, S.M., Houser, C., Nelson, F.E., 2011. Soil moisture: a central and unifying theme in physical geography. Prog. Phys. Geogr. 35 (1), 65–86.

Luo, Y., Sophocleous, M., 2010. Seasonal groundwater contribution to crop-water use assessed with lysimeter observations and model simulations. J. Hydrol. 389 (3–4), 325–335.

Maréchal, J.C., Dewandel, B., Subrahmanyam, K., 2004. Use of hydraulic tests at different scales to characterize fracture network properties in the weathered-fractured layer of a hard rock aquifer. Water Resour. Res. 40, 11.

Marquardt, D.W., 1963. An algorithm for least-squares estimation of nonlinear parameters. J. Soc. Ind. Appl. Math. 11 (2), 431–441.

McKenzie, N., Jacquier, D., Isbell, R., Brown, K., 2004. Australian soils and landscapes: an illustrated compendium. CSIRO Publishing.

Mishra, A.K., Singh, V.P., 2010. A review of drought concepts. J. Hydrol. 391 (1–2), 202–216.

Moriarty, P., Butterworth, J., van Koppen, B., Soussan, J., 2004. Water, poverty and productive uses of water at the household level. Beyond Domest. 19.

Mualem, Y., 1976. A new model for predicting the hydraulic conductivity of unsaturated porous media. Water Resour. Res. 12 (3), 513–522.

Mudrakartha, S., 2007. To adapt or not to adapt: The dilemma between long-term resource management and short-term livelihood. Agric. Groundw. Revolut.: Oppor. Threats Dev. 243–265.

Neumann, I., MacDonald, D., Gale, I. (2004). Numerical approaches for approximating technical effectiveness of artificial recharge structures. Commissioned Report CR/04/265N, British Geological Society, Keyworth, Nottingham, 46 pp.

Panda, D.K., Ambast, S.K., Shamsudduha, M., 2020. Groundwater depletion in northern India: impacts of the sub-regional anthropogenic land-use, socio-politics and changing climate. Hydrol. Process. https://doi.org/10.1002/hyp.14003.

Patidar, N., Keshari, A.K., 2020. A rule-based spectral unmixing algorithm for extracting annual time series of sub-pixel impervious surface fraction. Int. J. Remote Sens. 41 (10), 3970–3992.
Porporato, A., D'odorico, P., Laio, F., Ridolfi, L., Rodriguez-Iturbe, I., 2002. Ecohydrology of water-controlled ecosystems. Adv. Water Resour. 25 (8–12), 1335–1348.
Previati, M., Bevilacqua, I., Canone, D., Ferraris, S., Haverkamp, R., 2010. Evaluation of soil water storage efficiency for rainfall harvesting on hillslope micro-basins built using time domain reflectometry measurements. Agric. Water Manag. 97 (3), 449–456.
Rajasthan Ground Water Department (2008). Reappraisal of ground water resources of Udaipur District on 31.03.2007. Ground Water Department (GWD), Government of Rajasthan, Jodhpur, India.
Rangarajan, R., Athavale, R.N., 2000. Annual replenishable ground water potential of India—an estimate based on injected tritium studies. J. Hydrol. 234 (1–2), 38–53.
Rejani, R., Yadukumar, N., 2010. Soil and water conservation techniques in cashew grown along steep hill slopes. Sci. Hortic. 126 (3), 371–378.
Sakthivadivel, R., 2007. The groundwater recharge movement in India. Agric. Groundw. Revolut. Oppor. Threats Dev. 3, 195–210.
Sarah, S., Ahmed, S., Boisson, A., Violette, S., De Marsily, G., 2014. Projected groundwater balance as a state indicator for addressing sustainability and management challenges of overexploited crystalline aquifers. J. Hydrol. 519, 1405–1419.
Scanlon, B.R., Mukherjee, A., Gates, J., Reedy, R.C., Sinha, A.K., 2010a. Groundwater recharge in natural dune systems and agricultural ecosystems in the Thar Desert region, Rajasthan, India. Hydrogeol. J. 18 (4), 959–972.
Scanlon, B.R., Mukherjee, A., Gates, J., Reedy, R.C., Sinha, A.K., 2010b. Groundwater recharge in natural dune systems and agricultural ecosystems in the Thar Desert region, Rajasthan, India. Hydrogeol. J. 18 (4), 959–972.
Schaap, M.G., Leij, F.J., Van Genuchten, M.T., 2001. Rosetta: a computer program for estimating soil hydraulic parameters with hierarchical pedotransfer functions. J. Hydrol. 251 (3–4), 163–176.
Shah, T., 2007. The groundwater economy of South Asia: an assessment of size, significance and socio-ecological impacts. Agric. Groundw. Revolut.: Oppor. Threats Dev. 7–36.
Sharda, V.N., Kurothe, R.S., Sena, D.R., Pande, V.C., Tiwari, S.P., 2006. Estimation of groundwater recharge from water storage structures in a semi-arid climate of India. J. Hydrol. 329 (1–2), 224–243.
Sharma, O.P., Everard, M., & Pandey, D.N. (2018). Wise water solutions in Rajasthan. WaterHarvest/Water Wise Foundation, Udaipur, India.
Sheetal, S. (2012). Sustaining Groundwater: Role of Policy Reforms in Promoting Conservation in India. India Policy Forum. New Delhi: National Council of Applied Economic Research, pp. 1–33.
Šimůnek, J., van Genuchten, M.T., Šejna, M., 2005. The HYDRUS-1D software package for simulating the movement of water, heat, and multiple solutes in variably saturated media, version 3.0, HYDRUS software series 1. Department of Environmental Sciences, University of California Riverside, Riverside.
Šimůnek, J., Šejna, M., Saito, H., Sakai, M., Th Van Genuchten, M., 2008. The HYDRUS- 1D Software Package for Simulating the Movement of Water, Heat, and Multiple Solutes in Variably Saturated Media, Version 4.0, HYDRUS Software Series 3. Department of Environmental Sciences, University of California Riverside, Riverside, California, USA, p. 315.
Singh, R.B., Kumar, P., Woodhead, T., 2002. Smallholders Farmer in India: Food Security and Agricultural Policy. Food and Agriculture Organisation of the United Nations, Bangkok. https://coin.fao.org/coin-static/cms/media/9/13170962616430/2002_03_high.pdf.
Stiefel, J.M., Melesse, A.M., McClain, M.E., Price, R.M., Anderson, E.P., Chauhan, N.K., 2009. Effects of rainwater-harvesting-induced artificial recharge on the groundwater of wells in Rajasthan, India. Hydrogeol. J. 17 (8), 2061.
Van Genuchten, M.T., 1980. A closed-form equation for predicting the hydraulic conductivity of unsaturated soils. Soil Sci. Soc. Am. J. 44 (5), 892–898.
Vermote, Eric, NOAA CDR Program. (2019): NOAA Climate Data Record (CDR) of AVHRR Leaf Area Index (LAI) and Fraction of Absorbed Photosynthetically Active Radiation (FAPAR), Version 5. [/thredds/ncss/ncFC/cdr/lai-fapar-fc/LAI-FAPAR:_Aggregation_best. ncd]. NOAA National Centers for Environmental Information. https://doi.org/10.7289/V5TT4P69. Accessed [04/05/2020].
Villholth, K.G., 2006. Groundwater assessment and management: implications and opportunities of globalization. Hydrogeol. J. 14 (3), 330–339.
World Bank, 2010. Deep Wells and Prudence: Towards Pragmatic Action for Addressing Groundwater Overexploitation in India. The World Bank, Washington D.C.
Basant Yadav Alison Parker Anupma Sharma Rakesh Sharma Gopal Krishan Suraj Kumar Kristell Le Corre Pablo Campo Moreno Jaswant Singh Estimation of Groundwater Recharge in Semi-Arid Regions under Variable Land Use and Rainfall Conditions: A Case study of Rajasthan, India. PLOS Water.
Yang, L., Wei, W., Chen, L., Mo, B., 2012. Response of deep soil moisture to land use and afforestation in the semi-arid Loess Plateau, China. J. Hydrol. 475, 111–122.
Zaveri, E., Grogan, D.S., Fisher-Vanden, K., Frolking, S., Lammers, R.B., Wrenn, D.H., Nicholas, R.E., 2016. Invisible water, visible impact: groundwater use and Indian agriculture under climate change. Environ. Res. Lett. 11 (8), 084005.
Zucco, G., Brocca, L., Moramarco, T., Morbidelli, R., 2014. Influence of land use on soil moisture spatial temporal variability and monitoring. J. Hydrol. 516, 193–199.

# Assessment of traditional rainwater harvesting system in barren lands of a semi-arid region: a case study of Rajasthan (India)

Yadav, Basant

2022-06-25



Yadav B, Patidar N, Sharma A, et al., (2022) Assessment of traditional rainwater harvesting system in barren lands of a semi-arid region: a case study of Rajasthan (India). Journal of Hydrology: Regional Studies, Volume 42, August 2022, Article number 101149

https://doi.org/10.1016/j.ejrh.2022.101149